

# Large Kinetic Isotope Effects in Methane Oxidation Catalyzed by Methane Monooxygenase: Evidence for C–H Bond Cleavage in a Reaction Cycle Intermediate<sup>†</sup>

Jeremy C. Nesheim and John D. Lipscomb\*

Department of Biochemistry, Medical School, University of Minnesota, Minneapolis, Minnesota 55455

Received March 11, 1996; Revised Manuscript Received May 24, 1996<sup>®</sup>

**ABSTRACT:** The reduced hydroxylase component (MMOH) of soluble methane monooxygenase (MMO) from *Methylosinus trichosporium* OB3b reacts with O<sub>2</sub> and CH<sub>4</sub> to produce CH<sub>3</sub>OH and H<sub>2</sub>O in a single-turnover reaction. Transient kinetic analysis of this reaction has revealed at least five and probably six intermediates during the turnover [Lee, S.-K., Nesheim, J. C., & Lipscomb, J. D. (1993) *J. Biol. Chem.* 268, 21569–21577; Liu, Y., Nesheim, J. C., Lee, S.-K., & Lipscomb, J. D. (1995) *J. Biol. Chem.* 270, 24662–24665]. One intermediate, termed compound Q, reacts with CH<sub>4</sub> to yield enzyme-bound product. It is shown here that the deuterium kinetic isotope effect (KIE) for the reaction of compound Q with CH<sub>4</sub> is 50–100, which is one of the largest effects observed to date. The rate constants for the reactions of the deuterated homologs of methane decrease monotonically as the deuterium content increases, suggesting that a large primary isotope effect dominates. The KIEs determined by analyzing the products after a single turnover have the following values: 1:1 CH<sub>4</sub>:CD<sub>4</sub> (19); CD<sub>3</sub>H (12); CD<sub>2</sub>H<sub>2</sub> (9); and CH<sub>3</sub>D (4). The KIE values determined by directly observing the reactive intermediate and by monitoring product ratios are all large, consistent with complete C–H bond breaking in the oxygenation step of the reaction. However, the differences in the KIE values determined by these two methods suggest that the reaction is more complex than currently proposed. A modified mechanism introducing the possibility of hydrogen-atom reabstraction by an intermediate methyl radical is proposed.

Methane monooxygenase (MMO)<sup>1</sup> isolated from methanotrophic bacteria catalyzes the incorporation of one atom of oxygen from O<sub>2</sub> into an unactivated C–H bond of methane (bde = 104 kcal/mol, pK<sub>a</sub> = 48) to form methanol (Dalton, 1980; Lipscomb, 1994). The second atom of oxygen is reduced to water. Many other hydrocarbons serve as adventitious substrates (Higgins et al., 1980; Green & Dalton, 1989). The oxidation reaction of the soluble form of MMO occurs in the active site of the hydroxylase component (MMOH) of this three-protein-component enzyme system (Fox et al., 1989). The other two components are a NADH-coupled reductase (MMOR), which contains FAD and [Fe<sub>2</sub>S<sub>2</sub>] cofactors, and a cofactorless protein termed component B (MMOB) (Lund & Dalton, 1985; Fox et al., 1989, 1990b; Liu, Y., et al., 1995). MMOH contains a hydroxide-bridged diiron cluster that cycles between an activated diferrous state and a resting diferric state during each catalytic cycle (Ericson et al., 1988; Fox et al., 1988; Rosenzweig et

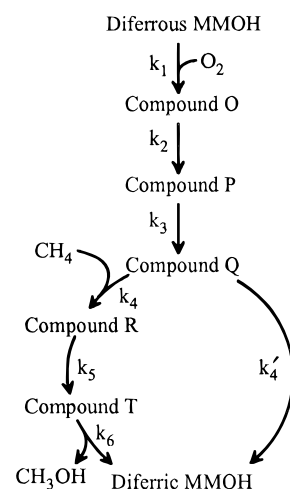


FIGURE 1: Sequence of reaction cycle intermediates in the single turnover of MMOH in the presence of MMOB.<sup>2</sup> The step labeled  $k_4'$  represents the first-order autodecay of compound Q, which occurs in the absence of substrates and may also occur in their presence.

<sup>†</sup> The work was supported by NIH Grant GM40466. J.C.N. was supported in part by NIH Training Grant GM08277.

\* Author to whom correspondence should be addressed.

<sup>®</sup> Abstract published in *Advance ACS Abstracts*, August 1, 1996.

<sup>1</sup> Abbreviations: bde, bond dissociation energy; D, <sup>2</sup>H; KIE, kinetic isotope effect; MMO, methane monooxygenase; MMOB, MMO component B; MMOH, MMO hydroxylase component; MMOR, MMO reductase component; MOPS, 3-morpholinopropanesulfonic acid.

<sup>2</sup> Recently an intermediate that formed with kinetic parameters of compound P was trapped and spectroscopically characterized by using hydroxylase from *Methylococcus capsulatus* (Bath) (Liu, K. E., et al., 1994, 1995a). This intermediate was termed compound L or the peroxy intermediate. The original nomenclature is maintained here for simplicity.

al., 1993; Woodland et al., 1986). Recently, as illustrated in Figure 1, we and others have shown that at least five, and probably six, transient intermediates occur as the diferrous MMOH cycles back to the diferic state after exposure to oxygen in the presence of MMOB and substrate (Lee et al., 1993b; Liu, K. E., et al., 1995a,b; Liu, Y., et al., 1995). One of these intermediates, termed compound Q, absorbs at 330 and 430 nm and exhibits an unusual Mössbauer spectrum best characterized as arising from a symmetric [Fe(IV)•Fe(IV)] state of the cluster (Lee et al., 1993a). Although

the structure of compound Q is not known, comparison of the Mössbauer spectral features with recently developed model systems suggests that there are two bridging  $\mu$ -oxo or hydroxo ligands forming a so-called "diamond core" structure (Que & Dong, 1996). The formation rate of compound Q is independent of substrate concentration for most substrates. In contrast, its decay rate is linearly dependent on substrate concentration, making the reaction appear second order overall. The rate constant for compound Q decay is strongly dependent on the particular MMO substrate added. Methane elicits the largest value among the many alkanes, alkenes, and heterocyclic compounds investigated so far. Chemical quench experiments indicate that product is formed in the active site at the same rate as compound Q decays. Together these observations suggest that compound Q reacts directly with substrate to form product and, thus, represents the form of the enzyme carrying the activated oxygen species capable of attacking unactivated hydrocarbon bonds.

Several potential mechanisms for the intriguing oxygen insertion reaction of the soluble MMO have been suggested. All of the proposals invoke direct coordination of oxygen to the diferrous cluster of MMOH to generate a peroxo adduct of some type, which is then cleaved homolytically or heterolytically to generate a radical or oxenoid reactive oxygen species, respectively. Barton and co-workers (Barton et al., 1992) have suggested that an iron oxenoid species might facilitate the formation of a bond between the iron and the substrate carbon to form a species that would allow direct insertion of oxygen. Feig and Lippard (1994) have suggested that an active site cysteine is oxidized by 1 reducing equiv by an oxenoid species to produce an active site diradical. In one proposed reaction from this species, concerted hydrogen atom abstraction by the cysteinyl radical and insertion by the cluster-associated oxygen radical would lead to product. Shteinman (1995) and Shestakov and Shilov (1996) have proposed that the diamond core structure of compound Q allows the redistribution of electron density, such that the irons are predominantly Fe(III) and each of the bridging oxygens has radical character. The coordinated attack of these radicals on substrate, one to carbon and one to hydrogen, is proposed to result in direct oxygen addition to the carbon to form a 5-coordinate methane intermediate that facilitates C–H bond breakage to yield product. We (Fox et al., 1989, 1990a; Froland et al., 1992; Priestley et al., 1992; Lipscomb, 1994) and others (Dalton et al., 1993) have speculated that a metal oxenoid species abstracts a hydrogen atom from the substrate to yield an intermediate substrate radical and a metal-bound hydroxyl moiety. Rebound of the hydroxyl would yield product. Considerable support for the latter mechanism has derived from experiments that showed that (*R*)- or (*S*)-[ $^2\text{H}_1, ^3\text{H}_1$ ]ethane undergoes partial inversion of configuration during the course of oxidation to ethanol, implying the formation of an unbound substrate-derived intermediate, probably a substrate radical, that can rotate in the active site before the reaction is consummated (Priestley et al., 1992).

Both the chemistry involved in the decay of compound Q and the proposed formation of an intermediate substrate radical can be investigated through the use of isotopically labeled methane. If we are correct in our proposals that the substrate oxidation chemistry of MMO occurs during compound Q decay, and that this chemistry involves complete

substrate C–H bond cleavage, then a substantial primary kinetic isotope effect in the decay of compound Q should result from deuteration of the methane. In contrast, the concerted reactions proposed in many of the other postulated mechanisms for MMO would not be expected to exhibit large primary KIEs. We demonstrate here that the oxidation of methane does show a large primary isotope effect. Indeed, the KIE is possibly the largest observed for any biological system reported to date, consistent with the hydrogen-atom abstraction mechanism for MMO.

## EXPERIMENTAL PROCEDURES

**Enzyme Preparation, Characterization, and Assay.** Bacterial growth and purification of MMO from *Methylosinus trichosporium* OB3b, as well as enzyme activity assays, were as reported previously (Fox et al., 1989, 1990b). MMO exhibited specific activity in the range of 600–800 nmol/min/mg for furan turnover. The temperature for assays was 23 °C, except in cases where a direct comparison with transient kinetic data was required. In these cases, the temperature was 4 °C. The buffer for all experiments was 100 mM MOPS, pH 7.7.

**Chemicals and Standard Procedures.** All reagents were the highest grade available and were obtained from Sigma, Aldrich, or EM Scientific. Deuterated gases were purchased from Cambridge Isotope Labs or ICON, and each was shown to be a single isotopic homolog (>99%) by mass spectrometric analysis. Water was deionized and glass distilled. Anaerobic techniques have been described previously (Fox et al., 1989).

**Stopped-Flow Absorption Spectroscopy Experiments.** MMOH (60  $\mu\text{M}$ , 120  $\mu\text{M}$  active sites) and methyl viologen (10  $\mu\text{M}$ ) were made anaerobic in 100 mM MOPS, pH 7.7. Sodium dithionite was added stoichiometrically (2 mol of reducing equivalents/mol of active sites) to reduce MMOH. MMOB was added anaerobically to a final concentration of 120  $\mu\text{M}$ . The enzyme solution was then loaded anaerobically into one stopped-flow syringe. The other stopped-flow syringe was loaded with oxygen-saturated buffer, with or without substrate. GC analysis of  $\text{CH}_4$ - or  $\text{CD}_4$ -saturated buffer or water at 23 °C showed the same dissolved methane concentration in all cases within experimental error. The concentration of a saturated solution was 1.5 mM (Merck Index). Single-turnover reactions by MMOH (4 °C) were followed by using a single-wavelength stopped-flow apparatus (Update Instruments, Inc.) at 430 nm.

**Data Analysis and Simulation.** The data were analyzed by using a nonlinear regression fitting program (KFIT, obtained from N. Millar, Kings College) to determine the formation and decay rates as previously described (Lee et al., 1993b). The slope of a plot of the observed rate constant versus substrate concentration is the second-order rate constant for the reaction. The ratio of the second-order rate constants for the reaction conducted with protiated and deuterated substrates gives the KIE. The data were analyzed as a straight line because, for methane and six other substrates examined, the compound Q decay rate is best fit as a linear function of substrate concentration. Over a much wider concentration range, the data may conform to the usual hyperbolic function; however, low solubility of substrates, and the steady decrease in the maximum amount of compound Q that can be observed as the decay rate increases, prevents examination of the kinetics at such high concentra-

tions. The data shown for compound Q kinetics with each of the five different isotopic homologs were obtained by measuring the rates of formation and decay of compound Q with at least five repetitions at each of four different methane concentrations. This entire procedure was repeated 2–5 times for each isotopic homolog.

The simulated curves shown in Figure 3 were calculated by assuming the rate of oxidation of a C–H bond in CH<sub>4</sub> to be equal to 3.9 s<sup>−1</sup>, which is equal to 25% of the overall rate of reaction of CH<sub>4</sub>. The calculated rate for compound Q decay in the presence of intermediately deuterated methanes was determined by summing the contributions of the H-abstraction process and the D-abstraction process to give the overall rate using the following equation:

$$\text{observed rate} = (3.9x)/(S^{4-x}) + 3.9(4-x)/(PS^{3-x})$$

where  $x$  is the number of hydrogens of the isotopic homolog,  $P$  is the primary isotope effect, and  $S$  is the secondary isotope effect (Bell, 1973).

**Product Yield Experiments.** Products were recovered from a single turnover of diferrous MMOH. The enzyme concentration, reduction procedures, and reaction conditions were as described earlier for stopped-flow experiments. The enzyme solution and a mixture of substrate (CH<sub>4</sub> and CD<sub>4</sub>, 640 μM; other isotopic homologs, 1.28 mM) and oxygen (200 μM) were loaded into separate stopped-flow syringes. A mechanical ram was used to push the solutions through a mixer and into a collection vial. The temperature was maintained at 4 °C.

**Methanol Derivatization.** The alcohol products produced by MMOH were first derivatized by the Schotten–Baumann procedure (Loudon, 1988). The reaction solution following the single turnover was added to CH<sub>2</sub>Cl<sub>2</sub> (50 mL) and then esterified using 3,5-dinitrobenzoyl chloride (2 mmol), *N,N*-dimethylaniline (2 mmol), and NaOH (2 mmol). The mixture was stirred for 17 h at room temperature. The organic layer was washed with 3 × 100 mL of HCl (1.0 M) followed by 3 × 100 mL of 5% NaHCO<sub>3</sub>–2 M NaCl, dried with anhydrous sodium sulfate, and evaporated to dryness, and the residue was dissolved in 2.0 mL of CH<sub>2</sub>Cl<sub>2</sub>. Thin-layer chromatography using silica gel plates and CHCl<sub>3</sub> as the mobile phase allowed separation of the methyl ester product at an  $R_f$  of 0.5–0.7. The area containing the product was scraped off and eluted with CH<sub>2</sub>Cl<sub>2</sub>. The CH<sub>2</sub>Cl<sub>2</sub> was evaporated to a minimal amount and the product was analyzed by mass spectrometry.

**Mass Spectrometric Analysis.** GC–MS was performed by using a Carlo-Erba gas chromatograph with a capillary DB-5 column, with direct injection into a Kratos MS-25 spectrometer. The retention times were determined using authentic material. The mass spectrometer was set to an ionization potential of 70 eV and selectively measured the molecular ion. Differential deuteration of the derivatized product resulted in partial separation of the two products on the GC column, necessitating the summing of multiple mass measurements (approximately 15) as the products eluted off the GC column. Each sample was analyzed in this way four times and the numbers were averaged. The isotope effect was calculated from the ratio of the products formed by H and D abstraction. Statistical factors were used when necessary to correct for different amounts of H and D of the substrate isotopic homologs.

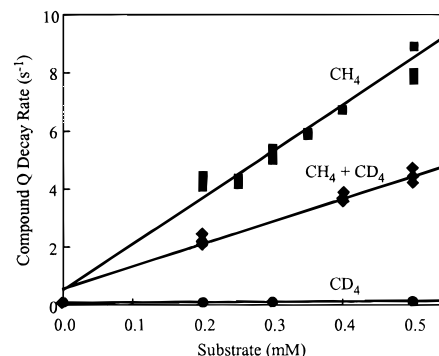


FIGURE 2: Effect of substrate concentration on compound Q decay rate constant. Shown are the pseudo-first-order rate constants of compound Q decay as a function of concentrations of CH<sub>4</sub> (■) and CD<sub>4</sub> (●) or a 1:1 mixture of CH<sub>4</sub> and CD<sub>4</sub> (◆).

**Steady State Kinetic Experiments.** The reaction rates were monitored by measuring the rates of oxygen consumption using a Clark-type oxygen electrode fitted to a reaction chamber sealed with a very small bore (<0.5 mm) glass stopcock to minimize the flux into and out of the reaction chamber. In all cases, the initial oxygen concentration was 250 μM. The methane concentration was varied from 10 μM to 1.2 mM by making appropriate additions of methane-saturated buffer to the reaction vessel. The total volume was held constant by the addition of nitrogen-saturated buffer. The concentrations of MMOH, MMOB, MMOR, and NADH were 370 nM, 925 nM, 375 nM, and 250 μM, respectively. The reaction was initiated by the addition of 1 μL of NADH solution and repeated 2–3 times for each of 10 different substrate concentrations. The buffer and temperature were the same as for the transient kinetic experiments, 100 mM MOPS, pH 7.7, at 4 °C.

## RESULTS

**Rate of Compound Q Decay in the Presence of Deuterated Methanes.** Compound Q formation and decay rates are easily determined by monitoring a single-turnover reaction at 430 nm using stopped-flow kinetic techniques and analyzing the data as described in Experimental Procedures. The rate of decay of compound Q is strongly dependent on the type and concentration of substrate present. Figure 2 shows the dependence of the compound Q decay rate constant on CH<sub>4</sub> and CD<sub>4</sub> concentrations. Each substrate caused a linear increase in the pseudo-first-order rate constant with increasing methane concentration. The slope of each line shown in Figure 2 gives the second-order rate constant for the reaction. Remarkably, the second-order rate constant for the CH<sub>4</sub> reaction is ~100 times greater<sup>3</sup> than that for the CD<sub>4</sub> reaction, indicative of an exceptionally large KIE. In contrast, no significant KIE or substrate concentration dependence was observed for the compound Q formation reaction.

The decay reactions were examined for artifacts that could lead to an apparent large isotope effect. Mixtures of CH<sub>4</sub> and CD<sub>4</sub> caused compound Q to decay in a single-exponential

<sup>3</sup> In assessing the rate constant for the CD<sub>4</sub> oxidation reaction, it is unclear whether the plot should be extrapolated to 0 rate at low substrate concentrations or to the autodecay rate ( $k'_d$ ). If the CD<sub>4</sub> oxidation occurs independently of the autodecay rate, then the CH<sub>4</sub>:CD<sub>4</sub> isotope effect is ~100. If the autodecay is prevented when substrates are present, then the isotope effect is ~50.

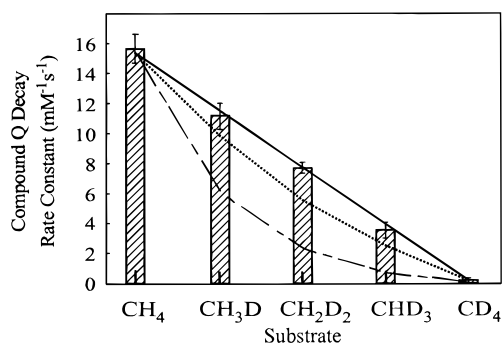


FIGURE 3: Compound Q second-order decay rate constants for differentially deuterated methane. Shown are the second-order rate constants for the reaction between compound Q and methane deuterated to various degrees. The second-order rate constant is obtained from the slope of the plot of compound Q decay rate constant versus methane concentration (see Figure 2). The solid line is drawn to highlight the linear trend with a primary KIE of 100 and a secondary KIE of 1. Error bars represent one standard deviation, data per point  $\geq 30$ . The broken lines are the results of simulations as described in Experimental Procedures. The parameters chosen for each simulation give an apparent KIE of  $\sim 100$ : (•••) A primary KIE of 60 and a secondary KIE of 1.2; (— —) a primary KIE of 12 and a secondary KIE of 2.

phase at the rate expected for the  $\text{CH}_4$  concentration present (Figure 2). This demonstrates that the  $\text{CD}_4$  samples used did not contain an inhibitor for the reaction and reinforces the observation that  $\text{CD}_4$  is essentially unreactive compared to  $\text{CH}_4$ . Also, it shows that the methane is in rapid equilibrium between the enzyme and the solvent, so that binding of the methane to (or collision with) the enzyme does not necessarily commit the reaction to completion.

The same experiment was carried out with mono-, di-, and trideuterated methanes with the second-order decay rate constants shown in Figure 3. The observed second-order rate constant decreases linearly with the extent of deuteration. Thus, the C–D bonds appear to be nearly inert to oxygen insertion in comparison with the C–H bonds.

**Temperature Dependence of Compound Q Decay in the Presence of Methane.** The activation energies and Arrhenius preexponential factors were measured for the reactions between compound Q and  $\text{CH}_4$  and  $\text{CD}_4$ . Since the reaction becomes very fast as the temperature is increased, the temperature range was limited from 1.8 to 7 °C for  $\text{CH}_4$  and from 2.5 to 16 °C for  $\text{CD}_4$ , when each was present at 300  $\mu\text{M}$  (Figure 4). The H and D activation energies are 22.4 and 24.5 kcal/mol, respectively, giving a difference of 2.1 kcal/mol with an overall error of  $\pm 10\%$ . The apparent Arrhenius preexponential factor ratio (H:D) is  $\sim 0.96$  (data not shown). The formation reactions showed the same activation energies (37.3 kcal/mol) and preexponential factors within experimental error.

**Effect of Methane Deuteration on Product Ratio from Compound Q Decay.** The methanol produced from a single turnover of diferrous MMOH was readily analyzed by GC–MS following derivatization as described in Experimental Procedures. Analysis of the results was simplified in some cases by the use of  $^{18}\text{O}_2$  in the oxygenation reaction, which served to shift the product mass by 2 units, so that it became distinct from the trace amounts of derivatized methanol originating from the extraction solvent. When  $\text{CD}_4$  and  $^{18}\text{O}_2$  were used as the substrates the only product was  $\text{CD}_3^{18}\text{OH}$ , showing that no exchange of oxygen or methyl hydrogens occurred. The results for the isotopic methane homologs

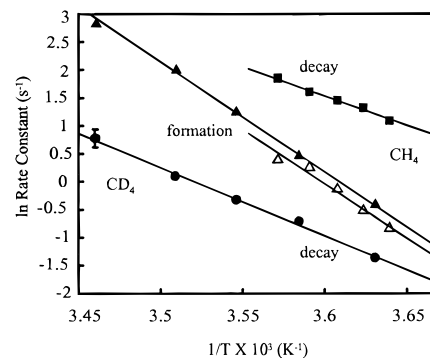


FIGURE 4: Temperature dependence of compound Q formation and decay rates during reaction with  $\text{CH}_4$  and  $\text{CD}_4$ . The reactions were carried out over temperature ranges of 1.8–7.0 and 2.5–16 °C for 300 mM  $\text{CH}_4$  and  $\text{CD}_4$ , respectively. The  $\text{CH}_4$ -mediated formation and decay rate constants of compound Q (■, △) and the respective  $\text{CD}_4$ -mediated rate constants (●, ▲) are shown. Observed error is within the dimensions of the symbol unless otherwise shown.

Table 1: Mass Spectrometric Analysis of the Derivatized Methanol Produced from a Single-Turnover Reaction of Diferrous MMOH<sup>a</sup>

substrate	KIE
$\text{CH}_4:\text{CD}_4$ (1:1)	$19.3 \pm 3.9^b$
$\text{CHD}_3$	$12 \pm 1$
$\text{CH}_2\text{D}_2$	$9.3 \pm 0.5^c$
$\text{CH}_3\text{D}$	$3.9 \pm 1^b$

<sup>a</sup> See Experimental Procedures for reaction and derivatization conditions. <sup>b</sup> In the reactions for  $\text{CH}_4:\text{CD}_4$  and  $\text{CH}_3\text{D}$ ,  $^{18}\text{O}_2$  was used instead of  $^{16}\text{O}_2$  to increase the mass of the product methanol by 2 units to make it distinguishable from trace amounts of contaminant methanol in the derivatization solutions. <sup>c</sup> A study utilizing the MMO system from *Methylococcus capsulatus* (Bath) gave a KIE for  $\text{CH}_2\text{D}_2$  turnover of 1.29 (Wilkins et al., 1994). We do not know the reason for this difference.

Table 2: Isotope Effects for  $\text{CH}_4$  and  $\text{CD}_4$  Oxidation Determined from Steady State Kinetic Parameters at 4 °C<sup>a</sup>

substrate	$V_{\max}$ (nmol/min/mg)	$K_M$ ( $\mu\text{M}$ )	$^D V_{\max}$	$^D(V_{\max}/K_M)$
$\text{CH}_4$	$72 \pm 6$	$12 \pm 2$		
$\text{CD}_4$	$45 \pm 4$	$184 \pm 4$	$1.6 \pm 0.3$	$25 \pm 5$

<sup>a</sup> Reaction conditions were as outlined in Experimental Procedures.

and mixtures of  $\text{CH}_4$  and  $\text{CD}_4$  are summarized in Table 1. The product ratios clearly reveal a large deuterium isotope effect in all cases. However, the intramolecular deuterium isotope effect is in the range of 4–13 rather than 50–100, as observed for compound Q decay rates. The largest value observed was 19.3 for the intermolecular isotope effect for a 1:1 mixture of  $\text{CH}_4$  and  $\text{CD}_4$ .

**Steady State Kinetics of Methane Turnover.** It has been reported by Rataj et al. (1991) that initial velocity measurements of  $\text{CH}_4$  and  $\text{CD}_4$  oxidation by the multiple-turnover reconstituted MMO system show that the major isotope effect appears in the  $V_{\max}:K_M$  ratio rather than in  $V_{\max}$ . This experiment was repeated under the same conditions used for the single-turnover studies (Table 2). In the case of methane turnover at 4 °C, the deuterium isotope effect in  $V_{\max}$  is  $1.6 \pm 0.3$ , while that for  $V_{\max}/K_M$  is  $25 \pm 5$ . The data are in accord with the study of Rataj et al. (1991), but different from the data reported for MMOH from *Methylococcus capsulatus* (Bath) by Wilkins et al. (1994). This study showed a  $V_{\max}$  isotope effect of 1.75, but an inverse isotope effect of 0.88 on the  $K_M$  and a  $V_{\max}/K_M$  isotope effect of 2.

## DISCUSSION

MMO presents a unique opportunity to utilize isotopic substitution to probe the oxygenase catalytic process because it is the only alkane oxygenase for which the reactive intermediate in the catalytic cycle has been directly monitored. In general, KIEs in monooxygenases such as cytochrome P450 and dopamine  $\beta$  monooxygenase must be measured by steady state kinetics or product analysis. Consequently, a direct measurement of the intrinsic isotope effect in the actual oxygen insertion step cannot be achieved and may be masked by slower steps such as product release or electron transfer (Gelb et al., 1982; Glickman et al., 1994; Hwang & Grissom, 1994; McMurphy & Groves, 1986; Northrop, 1975; Sugiyama & Trager, 1986). In the current study, we have shown that the decay of the reaction cycle intermediate compound Q, which appears to encompass the product-forming step, is very sensitive to the deuteration of methane. The mechanistic significance of this observation is discussed in the following sections.

*Origin of Unusually Large Isotope Effects.* The observed isotope effect for compound Q decay exceeds by severalfold the classical limit for a deuterium isotope effect. Large isotope effects typically arise in reactions that include (i) branched pathways, (ii) multiple steps with cumulative effects of more than one isotope-sensitive step, (iii) a hydrogen-tunneling process, or (iv) a magnetic isotope effect (Hwang & Grissom, 1994).<sup>4</sup> The effects of a branched reaction are usually seen in the product distribution rather than the direct observation of the decay of a reactive, chromophoric intermediate as reported here. The participation of more than one isotope-sensitive step is feasible, but the possibilities for such a process are constrained by the fact that no loss of hydrogen other than from the bond where oxygen insertion occurs is observed. Thus, it is unlikely that two hydrogen atoms are removed during the course of the reaction. In preliminary studies, we have not been able to observe magnetic isotope effects in the product distribution.<sup>5</sup> Consequently, of the possibilities noted, hydrogen tunneling appears to be the most likely origin of the large isotope effect.<sup>6</sup>

Observations characteristic of tunneling include (1) a large KIE  $> 7$ , (2) curvature in the Arrhenius plot, (3)  $\Delta\Delta H > 1.3$  kcal/mol, and (4) an Arrhenius preexponential factor ratio of  $A^H:A^D < 1$  (Brunton et al., 1976; More O'Ferrall, 1975). We have shown here that the compound Q decay reaction

in the presence of methane fulfills three of these criteria, in that it has a large KIE, a large difference in activation energies, and an apparent  $A^H:A^D$  of slightly less than 1. Curvature in the Arrhenius plot is not expected to be observable within the small temperature range that could be accessed in this study. Although tunneling is consistent with the data observed, under the assumption of tunneling both the apparent  $\Delta\Delta H$  and  $A^H:A^D$  will depend strongly on the temperature range in which the measurements are made. Thus, measurement of these parameters over a single small temperature range cannot be used to directly distinguish between tunneling and a classical Arrhenius mechanism.

Tunneling of the hydrogen atom during the abstraction process could elicit a large isotope effect, especially for a small, light molecule such as methane. Molecular orbital calculations of the hydrogen-atom abstraction process for methane have been carried out by Pudzianowski and Loew (1983). An intramolecular deuterium isotope effect for  $\text{CH}_3\text{D}$  of 34 was calculated for the process in the absence of tunneling and was 56 when a tunneling factor was added. The calculated  $\Delta G$  was very small,  $-0.2$  kcal/mol (298 K). Significantly, results from this computational experiment indicate that methane has a uniquely large KIE compared to the other hydrocarbons examined. These calculations<sup>7</sup> assumed that the hydrogen-atom abstraction was carried out by a ground state triplet oxygen atom and predicted a linear transition state with complete C–H bond fissure, as we have proposed for the mechanism of MMO.

A factor that can elevate the apparent KIE is differential solvation of the H- and D-atoms on the substrate (Pal et al., 1995). Due to the highly ordered solvent "cage" surrounding the hydrophobic substrate, the deuterium could be less easily accessed by the reactive oxidant than hydrogen. This type of effect is not related to the transition state. We discount this process as a significant contributor for our reactions because the second-order rate constants for  $\text{CH}_4$  and  $\text{CD}_4$  are essentially independent of the fraction of  $\text{D}_2\text{O}$  in the solvent.<sup>8</sup> The slight decrease observed can be accounted for entirely by the effects of the increased viscosity of  $\text{D}_2\text{O}$  on a collisional reaction.

Differences in partitioning of deuterated and protiated methane between the solvent and the hydrophobic interior of the enzyme might also cause anomalously large isotope effects. However, intramolecular isotope effects for the isotopic homologs of methane should not be affected by such bulk partitioning.

*Comparison of the Isotope Effects Determined from Compound Q Decay and from Product Distribution.* The deuterium isotope effects determined from product ratios, although large, are not as large as those determined directly from the kinetics of compound Q decay. In a single-turnover system, this would not normally be expected if compound Q reacts with substrate directly to form product as we propose. One possible explanation is that the reaction cycle

<sup>4</sup> Large isotope effects have also been reported for formation of a metal–hydrogen bond (Whitesides & Neilan, 1975) and H-atom abstraction by a peroxide radical (Howard et al., 1968). We currently cannot evaluate these possibilities for MMO.

<sup>5</sup> We have looked without success for magnetic isotope effects in the product ratios of  $\text{CH}_2\text{D}_2$  and  $\text{CHD}_3$  turnover in the range 0–0.4 T. It is reasonable to expect an effect in this field range based on the proposal that a diradical pair is generated in the active site. However, the observation of a magnetic isotope effect requires that the chemical reaction under study occurs within a time domain similar to or slower than that required for intersystem spin crossing,  $10^{-6}$ – $10^{-10}$  s (Grissom, 1995). Our previous results have indicated that the rebound rate for the putative radical pair is far faster than this range (Priestley et al., 1992).

<sup>6</sup> Recently, Klinman and co-workers (Glickman et al., 1994) and Grissom and co-workers (Hwang & Grissom, 1994) have reported a large isotope effect monitored by steady state kinetic techniques for soybean lipoxygenase turnover of linoleic acid. In this case, many possible hypotheses for the large isotope effect were investigated, but hydrogen tunneling was selected as the most reasonable.

<sup>7</sup> These calculations were carried out using the MNDO (modified neglect of diatomic overlap) protocol (Dewar & Thiel, 1977). This protocol is subject to several types of errors, including overestimation of the transition state enthalpy. This study warrants reinvestigation using more recent molecular orbital calculation strategies.

<sup>8</sup> In ongoing studies, we have shown that the KIE for compound Q decay in the presence of  $\text{CH}_4$  or  $\text{CD}_4$  is insensitive to substitution of  $\text{D}_2\text{O}$  for  $\text{H}_2\text{O}$  (J. C. Nesheim and J. D. Lipscomb, unpublished observation).

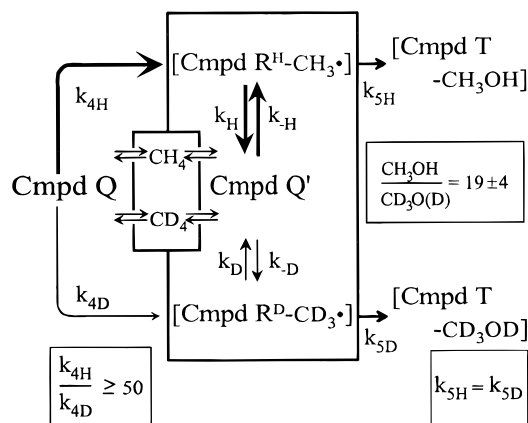


FIGURE 5: Hypothetical scheme to account for observed isotope effects in MMOH turnover.

branches before compound Q, so that only a small fraction of the reaction proceeds with an isotope effect approaching 100. This seems unlikely because it is known from Mössbauer spectroscopy that compound Q is formed by at least half, and probably significantly more than half, of the MMOH sites after reaction with  $O_2$  (Lee et al., 1993a). Also, the extinction coefficient of compound Q was estimated to be  $7500 \text{ M}^{-1} \text{ cm}^{-1}$  at 430 nm on the basis of the assumption that all of the observed product is formed via compound Q (Lee et al., 1993b). If this is not the case, then the extinction coefficient of compound Q is much larger than  $7500 \text{ M}^{-1} \text{ cm}^{-1}$ , which seems unlikely for a non-heme iron complex containing only two irons. A branch in the reaction pathway after the decay of compound Q would not alter the observed isotope effect unless it introduces a reversal of the hydrogen-atom abstraction. It is this possibility and the frequent correlation between a large primary KIE and a free energy change within several kilocalories/mole of zero [Bell (1973) and references cited therein] that leads us to put forth the scheme illustrated in Figure 5.

In this scheme, compound Q reacts with methane with a very large deuterium isotope effect. It is further proposed that the intermediate methyl radical can react by either reabstracting the original hydrogen atom or abstracting hydroxyl radical to complete the oxidation reaction. If the hydrogen atom is reabstracted, a different form of compound Q, designated Q', is proposed to form. This scheme would decrease the observed isotope effect in the product distribution because the hydrogen-atom reabstraction reaction would also show an isotope effect, while it is reasonable to assume a negligible isotope effect for the radical recombination process involving OH(D). Accordingly, the methane molecules that had lost deuterium would have a greater tendency to go on to product than those that had lost hydrogen, resulting in a lowering of the isotope effect as seen in the product analysis. Simulations of this scheme show that it models both the isotope effects determined from the kinetics of compound Q decay and from product yield if the reabstraction isotope effect is about 10 and the abstraction isotope effect for compound Q' is in the range of 10–100. However, there are many other values for these constants that also give good fits to the data. The reaction scheme requires that the methane generated by hydrogen-atom reabstraction in the active site exchange freely with methane in solution because if this were not the case, no isotope effect would be observed when a 1:1 mixture of  $CH_4$  and  $CD_4$

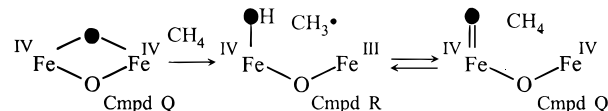


FIGURE 6: Possible structures for intermediate species shown in Figure 5.

reacts with compound Q. The reaction scheme also requires that compounds Q and Q' be discrete species because if this were not the case, the isotope effect in the decay rate of compound Q would remain correlated with the product isotope effect. Moreover, according to the scheme, compound Q decay should occur in at least three exponential phases. However, only one phase is observed, suggesting either that all species except compound Q are colorless at 430 nm (like the final species, diferric MMOH) and/or that compound Q' reacts with methane much faster than does compound Q. In either case, compound Q' would necessarily be distinguishable from compound Q.

The structures of the intermediate compounds Q, R, and the proposed intermediate Q' are not known. However, studies of high-valent model compounds (Dong et al., 1995a,b), as well as spectroscopic (Shu et al., 1996) and crystallographic (Rosenzweig et al., 1993, 1995) studies of the diferric hydroxylase, are consistent with a di- $\mu$ -oxo (or hydroxo) diiron cluster for compound Q. One scenario that could provide a structural basis for the scheme shown in Figure 5 is illustrated in Figure 6. In this case, the initial hydrogen abstraction by compound Q leads to the formation of a terminal hydroxo moiety, compound R, which, following the reabstraction reaction (compound Q'), does not rapidly reform the second oxo bridge. The resulting terminal oxenoid species would be expected to be at least as reactive as the dibridged structure, but might have significantly different spectroscopic properties as required by the data.

Although the hydrogen-atom reabstraction process is unexpected and has not been proposed for any other hydrocarbon-oxidizing system to our knowledge, the isotope effects determined from compound Q decay and the product ratio were both measured by straightforward techniques, suggesting that some process of this type does, in fact, occur. It is possible that the formation of a methyl radical presents a unique case in that it is expected to be significantly more reactive than other hydrocarbon radicals in the active site of MMO due to either the higher bde of the methane C–H bond or the potentially greater access of the methyl radical to the active site diiron cluster. The apparent occurrence of an isotope effect in two discrete steps means that MMO substrates other than methane may exhibit different isotope effects in either or both steps. Thus, the compound Q decay isotope effect might be larger or smaller than the product isotope effect for specific substrates.

**Secondary Isotope Effects.** Both the rate constant of compound Q decay and the KIE monitored by product formation show essentially linear changes with a change in deuterium content of the methane. However, the implications of these changes are different. In the case of compound Q decay, the linear plot suggests that the primary isotope is large and the secondary isotope effect is small. This is an important observation because an apparent KIE of  $\sim 100$  would be observed for a system with a more typical primary isotope effect (e.g., 12) and an exceptionally large secondary

effect (e.g. 2).<sup>9</sup> However, if this were the case, the plot shown in Figure 3 would be distinctly nonlinear. A simulation of the expected plot with a primary isotope effect of 60 and a secondary effect of 1.2 (apparent KIE = 100, Figure 3) is still slightly outside of the uncertainty in the data, suggesting that a maximum secondary isotope effect of ~1.1 would be allowed. In the case of the KIE monitored by product formation, there is a substantial decrease in the KIE as the deuterium content decreases. If the primary and secondary isotope effects were constant, then each of the isotopic homologs would give the same observed intramolecular isotope effect (given by the primary to secondary effect ratio); thus, the observed decrease is unexpected. A similar trend was noted for zirconium activation of methane C–H bonds by Wolczanski and co-workers (Schaller et al., 1994), who attributed the change to relatively large secondary isotope effects that differed for each isotopic homolog. In considering these two sets of data together, it appears that the secondary isotope effects have little or no effect on the compound Q decay rate, but a complex and much more significant effect on the observed product KIE. This supports a scheme, such as that shown in Figure 5, in which the observed effects derive from different reactions.

**Mechanistic Significance.** A deuterium isotope effect ranging from 4 to 20 is observed for both the product yield from methane single turnover by diferrous MMOH and the  $V_{\max}/K_M$  value determined from multiple turnover by the reconstituted system. Significantly, little isotope effect is observed in the  $V_{\max}$  value for steady state turnover. These observations are generally in accord with the proposed mechanism for MMOH. Transient kinetic experiments (Lee et al., 1993b) show the following: (i) all of the steps in the cycle leading to compound Q are effectively irreversible; (ii) compound Q forms before methane reacts productively with the enzyme; (iii) methane appears to react with compound Q without prior complex formation; and (iv) once methane reacts with compound Q, the product stays bound in the active site to be released slowly in the rate-limiting step. Under these constraints for either a sequential or nonsequential mechanism,  $V_{\max} \approx k_6 E_{\text{Total}}$  and  $K_{M,\text{CH}_4} \approx k_6/k_4$  (Segel, 1975). The product release step ( $k_6$ ) would not be expected to be isotope sensitive, and thus the observation of almost no isotope effect on  $V_{\max}$  is consistent with the mechanism shown in Figure 1. Similarly, the mechanism predicts the observed large isotope effect on  $K_M$  because the step in which the C–H bond-breaking chemistry occurs ( $k_4$ ) appears in the expression for this kinetic constant.

Various mechanistic studies of MMO have provided information about the nature of the substrate intermediate during the oxygen insertion step of the catalytic cycle. Unfortunately, these studies do not support the same conclusion. A study using ultrafast radical clock substrates by Lippard and co-workers (Liu, K. E., et al., 1993) showed that, for the *M. capsulatus* MMO, no radical trapping occurred on a time scale for rearrangement of  $10^{-11}$  s, suggesting that no substrate radical is formed and obviating the need for a discrete C–H bond-breaking step. In contrast, we have shown that for the *M. trichosporium* MMO, partial inversion of configuration of chiral ethane occurs, strongly

suggesting that a substrate intermediate free to rotate in the active site, most reasonably a substrate radical, is generated (Priestley et al., 1992). The studies described here show that the methane oxygen insertion reaction occurs with inter- and intramolecular deuterium isotope effects that are greater than 4 and, perhaps, as large as 100 for the C–H bond-breaking step itself. These effects seem inconsistent with any model that does not propose a C–H bond-breaking step to form a discrete substrate intermediate prior to oxygen addition.

## ACKNOWLEDGMENT

We thank Thomas P. Krick for mass spectrometry measurements and Dr. H. P. C. Hogenkamp for many helpful discussions.

## REFERENCES

- Barton, D. H. R., Bévière, S. D., Chavasiri, W., Cshai, E., Doller, D., & Liu, W.-G. (1992) *J. Am. Chem. Soc.* **114**, 2147–2156.
- Bell, R. P. (1973) *The Proton in Chemistry*, 2nd ed., Cornell University Press, Ithaca, NY.
- Brunton, G., Griller, D., Barclay, L. R. C., & Ingold, K. U. (1976) *J. Am. Chem. Soc.* **98**, 6803–6811.
- Dalton, H. (1980) *Adv. Appl. Micro.* **26**, 71–87.
- Dalton, H., Wilkins, P. C., & Jiang, Y. (1993) in *Microbial Growth on C<sub>1</sub> Compounds* (Murrell, J. C., & Kelly, D. P., Eds.) pp 65–80, Intercept, Andover.
- Dewar, J. S., & Theil, W. (1977) *J. Am. Chem. Soc.* **99**, 4899–4906.
- Dong, Y., Fujii, H., Hendrich, M. P., Leising, R. A., Pan, G., Randall, C. R., Wilkinson, E. C., Zang, Y., Que, L., Jr., Fox, B. G., Kauffmann, K. E., & Münck, E. (1995a) *J. Am. Chem. Soc.* **117**, 2778–2792.
- Dong, Y., Que, L., Jr., Kauffmann, K., & Münck, E. (1995b) *J. Am. Chem. Soc.* **117**, 11377–11378.
- Ericson, A., Hedman, B., Hodgson, K. O., Green, J., Dalton, H., Bentsen, J. G., Beer, R. H., & Lippard, S. J. (1988) *J. Am. Chem. Soc.* **110**, 2330–2332.
- Feig, A. E., & Lippard, S. J. (1994) *Chem. Rev.* **94**, 759–805.
- Fox, B. G., Surerus, K. K., Münck, E., & Lipscomb, J. D. (1988) *J. Biol. Chem.* **263**, 10553–10556.
- Fox, B. G., Froland, W. A., Dege, J. E., & Lipscomb, J. D. (1989) *J. Biol. Chem.* **264**, 10023–10033.
- Fox, B. G., Borneman, J. G., Wackett, L. P., & Lipscomb, J. D. (1990a) *Biochemistry* **29**, 6419–6427.
- Fox, B. G., Froland, W. A., Jollie, D. R., & Lipscomb, J. D. (1990b) *Methods Enzymol.* **188**, 191–202.
- Froland, W. A., Andersson, K. K., Lee, S.-K., Liu, Y., & Lipscomb, J. D. (1992) *J. Biol. Chem.* **267**, 17588–17597.
- Gelb, M. H., Heimbrook, D. C., Malkonen, P., & Sligar, S. G. (1982) *Biochemistry* **21**, 370–377.
- Glickman, M. H., Wiseman, J. S., & Klinman, J. P. (1994) *J. Am. Chem. Soc.* **116**, 793–794.
- Green, J., & Dalton, H. (1989) *J. Biol. Chem.* **264**, 17698–17703.
- Grissom, C. B. (1995) *Chem. Rev.* **95**, 3–24.
- Higgins, I. J., Best, D. J., & Hammond, R. C. (1980) *Nature* **286**, 561–564.
- Howard, J. A., Ingold, K. U., & Symonds, M. (1968) *Can. J. Chem.* **46**, 1017–1021.
- Hwang, C.-C., & Grissom, C. B. (1994) *J. Am. Chem. Soc.* **116**, 795–796.
- Kirsch, J. F. (1976) in *Isotope Effects on Enzyme Catalyzed Reactions* (Cleland, W. W., O'Leary, M. H., & Northrop, D. B., Eds.) pp 100–121, University Park Press, Baltimore, MD.
- Lee, S.-K., Fox, B. G., Froland, W. A., Lipscomb, J. D., & Münck, E. (1993a) *J. Am. Chem. Soc.* **115**, 6450–6451.
- Lee, S.-K., Nesheim, J. C., & Lipscomb, J. D. (1993b) *J. Biol. Chem.* **268**, 21569–21577.
- Lipscomb, J. D. (1994) *Annu. Rev. Microbiol.* **48**, 371–399.
- Liu, K. E., Wang, D., Huynh, B. H., Edmondson, D. E., Salifoglou, A., & Lippard, S. J. (1994) *J. Am. Chem. Soc.* **116**, 7465–7466.

<sup>9</sup> The secondary deuterium isotope effect is generally less than 1.25 for reactions involving changes in hybridization, as we propose here, and significantly lower for other types of reactions (Kirsch, 1976).

- Liu, K. E., Johnson, C. C., Newcomb, M., & Lippard, S. J. (1993) *J. Am. Chem. Soc.* **115**, 939–947.
- Liu, K. E., Valentine, A. M., Qui, D., Edmondson, D. E., Appelman, E. H., Spiro, T. G., & Lippard, S. J. (1995a) *J. Am. Chem. Soc.* **117**, 4997–4998.
- Liu, K. E., Valentine, A. M., Wang, D., Huynh, B.-H., Edmondson, D. E., Salifoglou, A., & Lippard, S. J. (1995b) *J. Am. Chem. Soc.* **117**, 10174–10185.
- Liu, Y., Nesheim, J. C., Lee, S.-K., & Lipscomb, J. D. (1995) *J. Biol. Chem.* **270**, 24662–24665.
- Loudon, G. M. (1988) in *Organic Chemistry*, 2nd ed., pp 884–887, The Benjamin/Cummings Publishing Company, Menlo Park, CA.
- Lund, J., & Dalton, H. (1985) *Eur. J. Biochem.* **147**, 291–296.
- McMurry, T. J., & Groves, J. T. (1986) in *Cytochrome P-450 Structure, Mechanism, and Biochemistry* (Ortiz de Montellano, P. R., Ed.) pp 1–28, Plenum Press, New York.
- More O'Ferrall, R. A. (1975) in *Proton Transfer Reactions* (Caldin, E. F., & Gold, V., Eds.) pp 201–262, Chapman and Hall, London.
- Northrop, D. B. (1975) *Biochemistry* **14**, 2644–2651.
- Pal, H., Nagasawa, Y., Tominaga, K., Kumazaki, S., & Yoshihara, K. (1995) *J. Chem. Phys.* **102**, 7758–7760.
- Priestley, N. D., Floss, H. G., Froland, W. A., Lipscomb, J. D., Williams, P. G., & Morimoto, H. (1992) *J. Am. Chem. Soc.* **114**, 7561–7562.
- Pudzianowski A. T., & Loew, G. H. (1983) *J. Phys. Chem.* **87**, 1081–1085.
- Que, L., Jr., & Dong, Y. (1996) *Acc. Chem. Res.* **29**, 190–196.
- Rataj, M. J., Kauth, J. E., & Donnelly, M. I. (1991) *J. Biol. Chem.* **266**, 18684–18690.
- Rosenzweig, A. C., Frederick, C. A., Lippard, S. J., & Nordlund, P. (1993) *Nature* **366**, 537–543.
- Rosenzweig, A. C., Nordlund, P., Takahara, P. M., Frederick, C. A., & Lippard, S. J. (1995) *Chem. Biol.* **2**, 409–418.
- Schaller, C. P., Bonnano, J. B., & Wolczanski, P. T. (1994) *J. Am. Chem. Soc.* **116**, 4133–4134.
- Segel, I. H. (1975) *Enzyme Kinetics*, pp 544–560, Wiley-Interscience, New York.
- Shestakov, A. F., & Shilov, A. E. (1996) *J. Mol. Catal. A: Chem.* **105**, 1–7.
- Shteinman, A. A. (1995) *Russ. Chem. Bull.* **44**, 975–984.
- Shu, L., Liu, Y., Lipscomb, J. D., & Que, L., Jr. (1996) *J. Biol. Inorg. Chem.* (in press).
- Sugiyama, K., & Trager, W. F. (1986) *Biochemistry* **25**, 7336–7343.
- Whitesides, T. H., & Neilan, J. P. (1975) *J. Am. Chem. Soc.* **97**, 907–908.
- Wilkins, P. C., Dalton, H., Samuel, C. J., & Green, J. (1994) *Eur. J. Biochem.* **226**, 555–560.
- Woodland, M. P., Patil, D. S., Cammack, R., & Dalton, H. (1986) *Biochim. Biophys. Acta* **873**, 237–242.

BI960596W